

# Numerical Modeling of Pressure drop due to Single-phase Flow of Water and Two-phase Flow of Air-water Mixtures through Thick Orifices

Manmatha K. Roul<sup>#1</sup>, Sukanta K. Dash<sup>\*2</sup>

<sup>#</sup> Department of Mechanical Engineering,  
Bhadra Institute of Engineering & Technology, Bhadrak (India) 756113

<sup>\*</sup> Department of Mechanical Engineering,  
Indian Institute of Technology, Kharagpur (India) 721302

**Abstract**– Pressure drops through thick orifices have been numerically investigated with single phase flow of water and two-phase flow of air–water mixtures in horizontal pipes. Two-phase computational fluid dynamics (CFD) calculations, using Eulerian–Eulerian model have been employed to calculate the pressure drop through orifices. The operating conditions cover the gas and liquid superficial velocity ranges  $V_{sg} = 0.3\text{--}4$  m/s and  $V_{sl} = 0.6\text{--}2$  m/s, respectively. The local pressure drops have been obtained by means of extrapolation from the computed upstream and downstream linearized pressure profiles to the orifice section. Simulations for the single-phase flow of water have been carried out for local liquid Reynolds number ranging from  $3 \times 10^4$  to  $2 \times 10^5$  to obtain the discharge coefficient and two-phase local multiplier. The effect of orifice geometry on two-phase pressure losses has been considered by selecting two pipes of 60 mm and 40 mm inner diameter and four different orifice plates (for each pipe) with two area ratios ( $\sigma = 0.73$  and  $\sigma = 0.54$ ) and two different orifice thicknesses ( $s/d = 0.025, 0.59$ ). The results obtained from numerical simulations are validated against experimental data from the literature and are found to be in good agreement

**Keywords**– orifice, pressure drop, two phase flow, area ratio, discharge coefficient, two-phase multiplier.

## I. INTRODUCTION

Knowledge of pressure drop for single phase flows and two-phase flows through valves, orifices and other pipe fittings are important for the control and operation of industrial devices such as chemical reactors, power generation units, refrigeration apparatuses, oil wells, and pipelines. The orifice is one of the most commonly used elements in flow rate measurement and regulation. Because of its simple structure and reliable performance, the orifice is increasingly adopted in gas-liquid two-phase flow measurements. Single orifices or arrays of them constituting perforated plates, are often used to enhance flow uniformity and mass distribution downstream of manifolds and distributors. They are also used to enhance the heat-mass transfer in thermal and chemical processes (e.g. distillation trays). Single-phase flows across orifices have been extensively studied, as has been shown by Idelchik et al. [1] in their handbook. The available correlations do not always take into account Reynolds number effect and a

complete set of geometrical parameters. Some investigations have been made on the theory and experiment of resistance characteristics of orifices [1-4] and some useful correlations have been proposed. However, some of them cover only a limited range of operating conditions, and the errors of some are far beyond the limit of tolerance. So they are not widely used in engineering design. Major uncertainties exist with reference to two-phase flows through orifices. Few experimental studies reported in the literature often refer to a limited set of operating conditions. With particular reference to orifice plates, some of the correlations and models [2-4] are discussed by Roul and Dash [5]. Other references are the experimental study by Lin [6] on two-phase flow measurement with sharp edge orifices; the experimental investigation by Saadawi et al. [7], which refers to two-phase flows across orifices in large diameter pipes and the work by Kojasoy et al. [8] on multiple thick and thin orifice plates. Fossa and Guglielmini [9] experimentally investigated two-phase flow pressure drop through thin and thick orifices and observed that the void fraction generally increases across the singularity and attains a maximum value just downstream of restriction.

The information regarding the effects of orifice thickness on two-phase pressure losses is not available in the literature. In the present study the effect of orifice geometry on two-phase pressure losses has been considered by selecting two pipes of 60 mm and 40 mm inner diameter and four different orifice plates with two area ratios ( $\sigma = 0.73$  and  $\sigma = 0.54$ ) and two different thicknesses (one thin and one thick orifice) ( $s/d = 0.025, 0.59$ ). When the value of  $s/d$  is below 0.5 it is called a thin orifice otherwise it is a thick orifice [3]. The results presented in this study provide useful information on the reliability of available models and correlations when applied to intermittent flows through orifices having high values of the contraction area ratio.

## II. THEORETICAL BACKGROUND

### A. Single-phase Flow

For the flow through a thin orifice, the flow contracts with negligible losses of mechanical energy, to a vena contracta of

area  $A_c$  that forms outside the restriction. Downstream of the vena contracta the flow expands in an irreversible process to the pipe wall of flow area  $A$ .

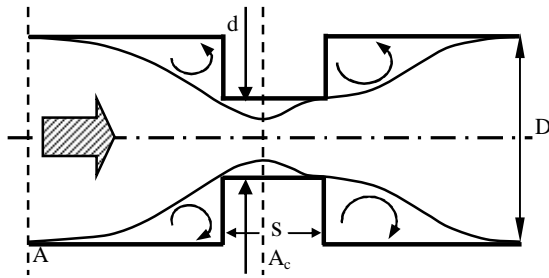


Fig. 1 Single-phase flow across thick orifices

If the orifice is thick (Fig. 1), downstream of the vena contracta, the flow reattaches to the wall within the length of the geometrical contraction and can even develop a boundary layer flow until it finally expands back into the pipe wall. According to Chisholm [3], the thick orifice behavior takes place when the dimensionless orifice thickness to diameter ratio,  $s/d$  is greater than 0.5. Assuming that each expansion occurs irreversibly and the fluid is incompressible, the single-phase pressure drop  $\Delta P$  in a thin orifice can be expressed as a function of the flow area ratio  $\sigma = (d/D)^2$  and the contraction coefficient  $\sigma_c = A_c/A\sigma$  as:

$$\Delta P_{sp} = \frac{\rho V^2}{2} \left[ \left( \frac{1}{\sigma \sigma_c} - 1 \right) \right]^2 \quad (1)$$

where  $\rho$  is the fluid density and  $V$  its mean velocity.

If the orifice is thick, the loss of mechanical energy is due to the double expansion as described above. For these conditions the single-phase overall pressure drop can be expressed as:

$$\Delta P_{sp} = \frac{\rho V^2}{2} \left[ \left( \frac{1}{\sigma \sigma_c} \right)^2 - 1 - \frac{2}{\sigma^2} \left( \frac{1}{\sigma_c} - 1 \right) - 2 \left( \frac{1}{\sigma} - 1 \right) \right] \quad (2)$$

The local pressure drop can also be expressed as a function of orifice discharge coefficient  $C_d$  (Lin [6], Grace and Lapple [10]):

$$\Delta P_{sp} = \frac{\rho V^2}{2} \left[ \left( \frac{1}{\sigma} \right)^2 - 1 \right] \frac{1}{C_d^2} \quad (3)$$

From Eqs. (1) and (3),  $\sigma_c$  for thin orifices can be written as:

$$\sigma_{c,thin} = \frac{1}{\sigma + \sqrt{1 - \sigma^2}/C_d} \quad (4)$$

Similarly from Eqs. (2) and (3),  $\sigma_c$  for thick orifices can be written as:

$$\sigma_{c,thick} = \frac{1}{1 + \sqrt{\left[ (1 - \sigma^2)/C_d^2 \right] - 1 + 2\sigma - \sigma^2}} \quad (5)$$

The well known Chisholm expression for contraction coefficient in terms of the area flow ratio only (Chisholm [3]) is given as:

$$\sigma_c = \frac{1}{\left[ 0.639(1 - \sigma)^{0.5} + 1 \right]} \quad (6)$$

In the present study the pressure drops across different orifices for single phase flow of water are obtained numerically, from which the discharge coefficient is calculated using Eq. (3). The contraction coefficient is calculated using Eqs. (4) and (5) for thin and thick orifices respectively. This contraction coefficient is compared with the Chisholm correlation as given by Eq. (6).

**B. Two-phase Flow**

According to Chisholm [3] and Morris [4], the slip ratio  $S$  is defined as the ratio of gas phase velocity to the liquid phase velocity at any point in the flow path (Collier and Thome [11]) and it is a function of the quality  $x$  and the ratio of fluid densities. When the quality of mixtures,  $x$  is very low (such as those considered in the present investigation,  $x < 0.005$ ), the slip ratio,  $S$  can be expressed as:

$$S = \left[ 1 + x \left( \frac{\rho_l}{\rho_g} - 1 \right) \right]^{0.5} \quad (7)$$

Where slip ratio,  $S$  is defined as the ratio of gas phase velocity to the liquid phase velocity at any point in the flow path (Collier and Thome [11]). The quality,  $x$  is defined as the ratio of mass flux of gas to the total mass flux of mixture at any cross-section [11]. The mass flux of gas is the gas mass flow rate divided by total cross-sectional area of pipe whereas the total mass flux is the total mass flow rate of mixture divided by total cross-sectional area of the pipe. Mathematically the quality  $x$  can be expressed as:

$$x = \frac{\rho_g g V_{sg} / A_{cross}}{\rho_g g V_{sg} / A_{cross} + \rho_l g V_{sl} / A_{cross}} = \frac{\rho_g V_{sg}}{\rho_g V_{sg} + \rho_l V_{sl}} \quad (8)$$

For fully developed flow, near atmospheric pressure, the slip ratio can be expressed in terms of the gas volume fraction:

$$x_v = V_{sg} / (V_{sg} + V_{sl})$$

$$S = \frac{1 - 0.833x_v}{0.833(1 - x_v)} \quad (9)$$

Kojasoy et al. [8] adopt the Chisholm expression for slip ratio  $S$  but they suggest a correction to account for the effect of flow restriction on slip ratio:

$$S = \left[ \left\{ 1 + x \left( \frac{\rho_l}{\rho_g} - 1 \right) \right\}^{0.5} \right]^n \quad (10)$$

The exponent  $n$  is zero at the vena contracta and downstream of it (i.e. the slip ratio is expected to be one) while  $n$  is equal to 0.4 and 0.15 in the upstream region for thin and thick orifices respectively.

Simpson et al. [2] adopted a different correlation for slip evaluation that does not account for the quality of the mixture:

$$S = \left( \frac{\rho_l}{\rho_g} \right)^{1/6} \quad (11)$$

The prediction of the two-phase multiplier,  $\Phi_{lo}^2$  can be calculated using different models as described below. The two-phase multiplier is defined as the ratio of the two-phase pressure drop through the orifice to the single-phase pressure drop obtained at liquid mass flux equal to the overall two-phase mass flux.

If the mixture can be considered homogeneous ( $S = 1$ ), the following expression can be obtained:

$$\Phi_{lo}^2 = \frac{\rho_l}{\rho_g} x + (1-x) \quad (12)$$

Chisholm [3] developed the following expression:

$$\Phi_{lo}^2 = 1 + \left( \frac{\rho_l}{\rho_g} - 1 \right) [Bx(1-x) + x^2] \quad (13)$$

where the parameter  $B$  can be assumed to be 0.5 for thin orifices and 1.5 for thick ones.

Morris relationship [4] refers to thin orifices and gate valves and has the following expression:

$$\Phi_{lo}^2 = \left[ x \frac{\rho_l}{\rho_g} + S(1-x) \right] \left[ x + \left( \frac{1-x}{S} \right) \left( 1 + \frac{(S-1)^2}{(\rho_l/\rho_g)^{0.5} - 1} \right) \right] \quad (14)$$

where, the slip ratio  $S$  is given by Eq. (7).

Simpson et al. [2] proposed the following relationship based on slip predictions given by Eq. (11):

$$\Phi_{lo}^2 = [1 + x(S-1)] [1 + x(S^5 - 1)] \quad (15)$$

Simpson model is based on data collected with large diameter pipes (up to 127 mm) at mixture qualities generally higher than those obtained in this work ( $x < 0.005$ ).

Finally the correlation of Saadawi et al. [7], based on experiments carried out at near atmospheric pressure with a very large diameter pipe (203 mm), is given by:

$$\Phi_{lo}^2 = 1 + 184x - 7293x^2 \quad (16)$$

In the present study the pressure drops across different orifices for two-phase flow of air-water mixtures are obtained numerically. The single-phase pressure drops at liquid mass flux equal to the overall two-phase mass flux are obtained by interpolating the single-phase pressure drop results. The two-phase multiplier is obtained by taking the ratio of the two-phase pressure drop to that of the single phase pressure drop. The two-phase multiplier thus obtained is compared with the theoretical predictions from the above equations (Eqs. (12)–(16)).

### III. NUMERICAL MODELING

The governing equations of mass, momentum and turbulent quantities have been integrated over a control volume and the subsequent equations have been discretized over the control volume using the finite volume technique (Patankar [12]) to yield a set of algebraic equations. Boundary conditions were implemented to the finite volume equations which could be solved by the algebraic multigrid scheme of Fluent 6.3. The flow field was assumed to be axisymmetric and solved in two

dimensions. The algebraic equations were solved using double precision solver with an implicit scheme for all variables with a variable time step starting at 0.00001s and finally going up to 0.001s for quick convergence. The discretization scheme for momentum, volume fraction, turbulent kinetic energy and turbulent dissipation rate were taken to be first order up winding initially for better convergence. Slowly as time progressed the discretization forms were switched over to second order up winding and then slowly towards the QUICK scheme for better accuracy. It is to be noted here that in the Eulerian scheme of solution, two continuity equations and two momentum equations were solved for two phases. The Phase-Coupled SIMPLE algorithm (Vasquez and Ivanov [13]), which is an extension of the SIMPLE algorithm (Patankar [12]) for multiphase flows was used for the pressure-velocity coupling. The velocities were solved coupled by the phases, but in a segregated fashion. Then a pressure correction equation was built based on total volume continuity rather than mass continuity. Pressure and velocities were then corrected so as to satisfy the continuity constraint. The Reynolds stress model (RSM) has been used as a closure model for turbulent flow. Abandoning the isotropic eddy-viscosity hypothesis, the RSM closes the Reynolds-averaged Navier-Stokes equations by solving transport equations for the Reynolds stresses, together with an equation for the dissipation rate. This means that five additional transport equations are required in 2D flows. The two-layer model for enhanced wall treatment was used to account for the viscosity-affected near-wall region in numerical computation of turbulent flow. Fine grids were used near the wall as well as near the orifice, where the mean flow changes rapidly and there are shear layers with a large mean rate of strain. The scaled residuals for continuity, velocity of water and air in axial and radial directions, and for water, uu-water, vv-water, ww-water, uv-water and volume fraction for air were monitored. The convergence criteria for all the variables were taken to be 0.001. If the residuals for all problem variables fall below the convergence criteria but are still in decline, the solution is still changing, to a greater or lesser degree. A solution is said to be truly converged if the scaled residuals are no longer changing with successive iterations. A better indicator occurs when the residuals flatten in a traditional residual plot (of residual value vs. iteration). Convergence was judged not only by examining scaled residual levels, but also by monitoring the velocities and pressures at three different locations very close to the orifice section (at 5D upstream, at the orifice and at 5D downstream). The solution was considered to have converged when there was no further observable change in the velocity and pressure at each location. Finally it was observed that the scaled residual for continuity equation was below  $10^{-3}$  and that for all other variables were well below  $10^{-6}$ .

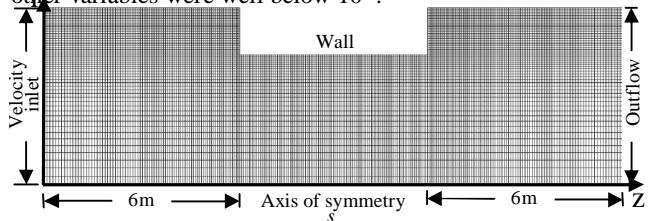


Fig. 2 Computational domain for  $\sigma = 0.54$ ,  $s/d = 0.59$  and  $D = 40\text{mm}$ . Velocity inlet boundary condition is applied at the inlet (as shown in Fig. 2). A no-slip and no-penetrating boundary condition is imposed on the wall of the pipe and the two-layer model for enhanced wall treatment was used to account for the viscosity-affected near-wall region. At the outlet, the boundary condition is assigned as outflow, which implies diffusion flux for the entire variables in exit direction are zero. Symmetry boundary condition is considered at the axis, which implies normal gradients of all flow variables are zero and radial velocity and the shear stress are zero at the axis.

Fig. 2 shows the domain used for the area ratio of 0.54, orifice thickness to diameter ratio of 0.59 in 40 mm diameter pipe (half of the section is modeled, with a symmetry boundary at the centerline). Numerical mesh used for different values of  $s/d$ , area ratio and pipe diameter, were determined from several numerical experiments which showed that further refinement in grids in either direction did not change the result (maximum change in pressure drop or any scalar variable) by more than 1%.

IV. RESULTS AND DISCUSSIONS

Two different horizontal pipes are considered, having inner diameters  $D$  equal to 60 mm and 40 mm. The test section is about 12 m long. The orifice is located 6 m downstream the inlet section. The effect of orifice geometry has been considered by selecting 8 different orifices. The 8 shapes here result from two pipe diameters ( $D = 60$  mm and 40 mm), two area ratios ( $\sigma = 0.73$  and 0.54) and two orifice thicknesses, ( $s/d = 0.025$  and 0.59). According to Chisholm [3] criteria the orifice having  $s/d = 0.59$  can be classified as a “thick” orifice. The fluids used are air and water at room temperature and near atmospheric pressure. Gas superficial velocities are taken in the range  $V_{sg} = 0.3\text{--}4$  m/s, while liquid superficial velocities are taken in the range  $V_{sl} = 0.6\text{--}2$  m/s.

The local pressure drops have been obtained by extrapolating the computed pressure profiles upstream and downstream of the orifice (in the region of fully developed pipe flow) to the orifice section as demonstrated in fig 3. For fully developed flow in upstream and downstream of the orifice section the variation of static pressure with length of the pipe ( $L/d$ ) is linear.

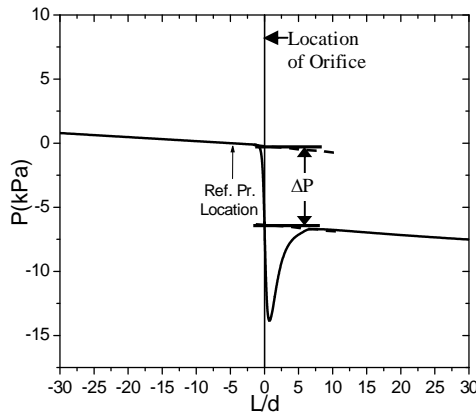


Fig. 3 Pressure drop at the orifice section by extrapolating the upstream and downstream pressure profiles are extrapolated to the orifice section as shown in figure 3, from which the pressure drop at the orifice section is calculated. Local pressure drop means the pressure drop at the orifice section. The reference pressure is located at a distance of  $5d$  from the orifice section in the upstream direction, where  $d$  is the diameter of the orifice. The pressure at this location is taken as the atmospheric pressure or zero gauge pressure. If the pressure at any section is more than the reference pressure then it is positive or else it is negative as can be seen from figure 3. The position of the orifice is taken as the origin and the upstream distances are taken as negative where as the downstream distances are taken as positive.

The procedure is repeated for single-phase flow of water and two-phase flow of air-water mixtures in order to compute the two-phase multiplier  $\phi_{io}^2$ .

A. Single-phase Flow

The velocity vectors and stream lines for single phase water flow through orifices having  $s/d = 0.025$  and 0.59 are shown in Figs. 4 and 5 respectively. It is evident from the figures that for the flow through thin orifices ( $s/d = 0.025$ ), the flow contracts to a vena contracta that forms outside the restriction. At the vena contracta the flow becomes parallel and downstream of the vena contracta the flow expands to the pipe wall of flow area A. A region of separated flow occurs from the sharp corner of the orifice and extends past the vena contracta. For the flow through thick orifice ( $s/d = 0.59$ ), vena contracta always forms inside the restriction. Downstream of the vena contracta, the flow reattaches to the wall within the length of the geometrical contraction and it finally expands back into the pipe wall. Simulated velocity vectors clearly show that eddy zones are formed in the separated flow region. The pressure profiles for the single phase flow of water through orifice  $s/d = 0.59$  in 40 mm diameter pipe for area ratio,  $\sigma = 0.54$  are shown in Fig. 6 as a function of Reynolds number,  $Re_d$ . The liquid Reynolds number is defined as:

$$Re_d = Gd/\mu_l$$

where  $G$  is the total mass flux corresponding to orifice section,  $d$  is the orifice diameter, and  $\mu_l$  is the viscosity of liquid. It is observed that the static pressure attains the (locally) smallest value at a distance of about  $z'/d = 0.5$  after the orifice section and depends only slightly on the mass flow rates. For the same  $s/d$  value the axial pressure drop at the orifice section increases with increase in  $Re_d$  number.

Figure 7 shows the pressure profile for single phase flow of water through orifices of different thickness for  $Re_d = 200000$ . It clearly shows that the pressure drop,  $\Delta P$  across the orifice increases with a decrease in orifice thickness and pressure drop decreases with an increase in area ratio. For the same pipe diameter, when the area flow ratio decreases, orifice diameter also decreases. When expansion takes place from smaller diameter to larger diameter, the height of the

recirculation zone increases. This results in the formation of more vortices and hence more pressure drop will occur.

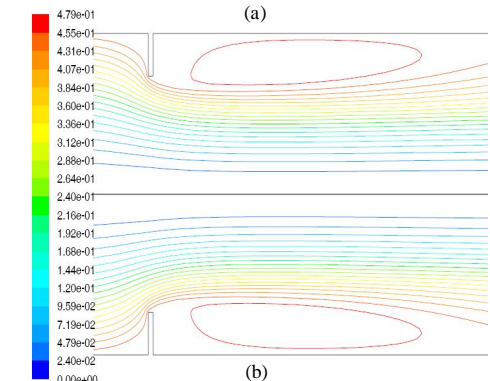
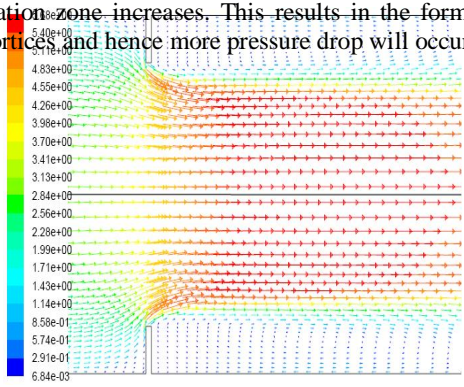


Fig. 4 (a) Velocity vectors and (b) Stream lines for single phase water flow through orifice  $\sigma = 0.54$ ,  $s/d = 0.025$ , and  $D = 40$  mm

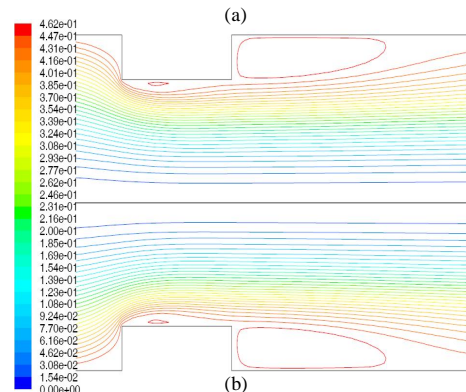
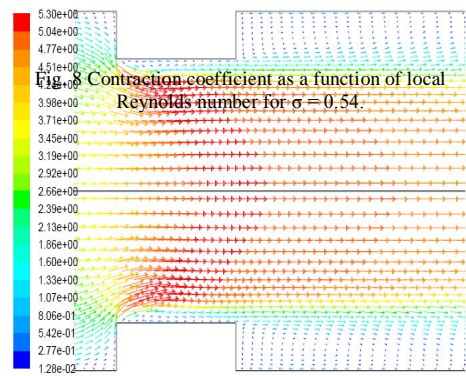


Fig. 5(a) Velocity vectors and (b) Stream lines for single phase water flow through orifice  $\sigma = 0.54$ ,  $s/d = 0.59$ , and  $D = 40$  mm

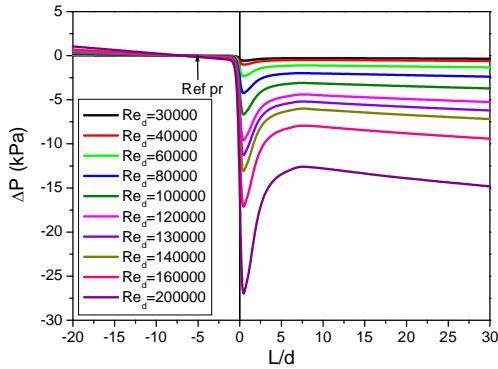


Fig. 6 Pressure profiles for single phase water flow through  $D = 40$  mm,  $\sigma = 0.54$ ,  $s/d = 0.59$  orifice

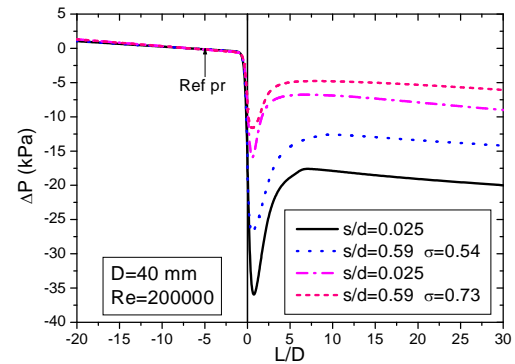
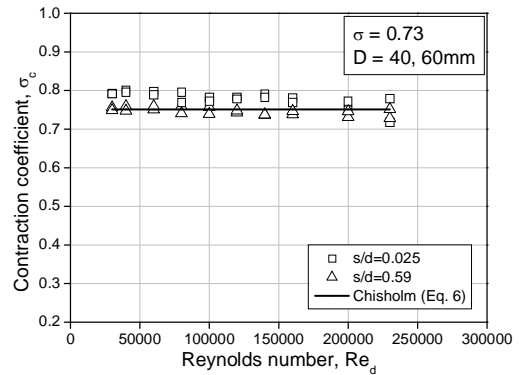
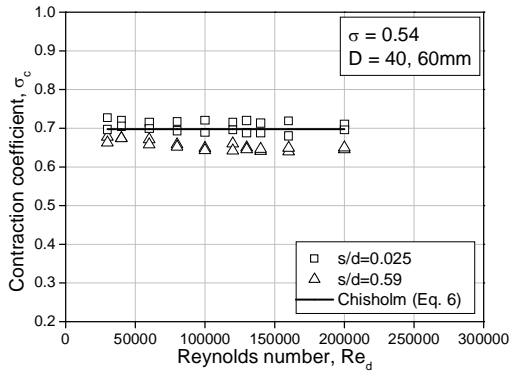


Fig. 7 Pressure profiles for single phase water flow through different orifices



From the computed pressure profiles upstream and downstream of the orifice, the local pressure drop has been obtained by extrapolating these profiles to the orifice section. From the local pressure drop values the orifice discharge coefficient  $C_d$  is calculated, from which the contraction coefficient  $\sigma_c$  has been obtained by means of Eqs. (3)–(5). Figs. 8 and 9, which refer to either the 60 mm or 40 mm diameter pipe show the  $\sigma_c$  values as a function of restriction Reynolds number,  $Re_d$  for different values of the flow area ratio. It can be observed from figures 8 and 9 that the contraction coefficient turns out to be independent of the Reynolds number for values above  $5 \times 10^4$ . For lower values of Reynolds number, the contraction coefficient generally increases with it. Finally it can be noticed that the contraction coefficient data are in good agreement with Chisholm formula predictions (Eq. (6)). The contraction coefficient is high (around 0.76) for area flow ratio of 0.73, whereas that for area flow ratio of 0.54, is around 0.7. This is because for higher area flow ratio, the orifice diameter is more and so the height of the recirculation zone is smaller and hence the pressure drop is less. From equation (3) it can be observed that when  $\Delta P$  is less,  $C_d$  is more and from equation (4) it can be observed that when  $C_d$  is more,  $\sigma_c$  is more.

Fig. 10 shows the effect of orifice thickness on the local pressure drop during the single-phase flow of water. It clearly shows that local pressure drop increases with increase in Reynolds number and for the same value of Reynolds number local pressure drop is less for thick orifices. With turbulent flows through orifices the contraction coefficients are found to be slightly higher for contraction area ratio  $\sigma = 0.73$  than that for  $\sigma = 0.54$ .

**B. Two-phase Flow**

The pressure loss due to two-phase flow of air-water mixtures through orifice is calculated from computed upstream and downstream pressure gradients. The procedure is based on the assumption that the orifice does not affect the pressure profiles with respect to the unrestricted flow. Pressure drop for two-phase air-water flow through the orifice having  $s/d = 0.025$  and  $s/d = 0.59$  in 60 mm diameter pipe for  $\sigma = 0.73$  and  $\sigma = 0.54$  are shown in Fig. 11a and b respectively for a constant

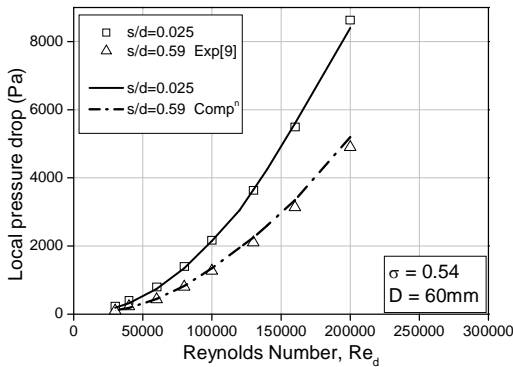


Fig. 10 Single-phase pressure drop as a function of local Reynolds number for  $\sigma = 0.54$ .

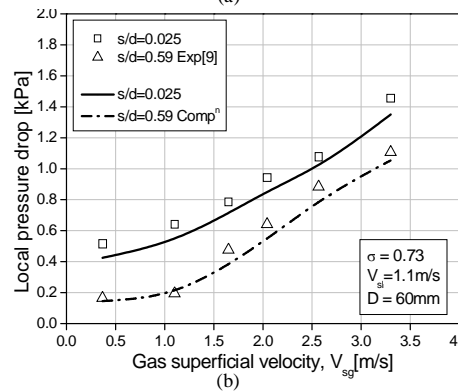
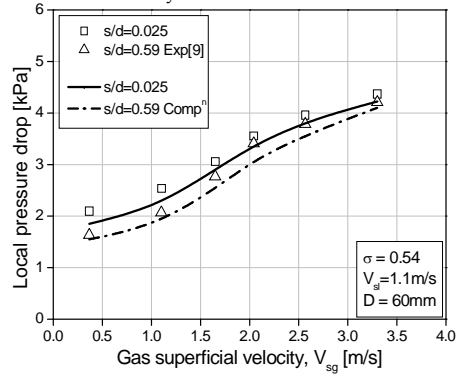
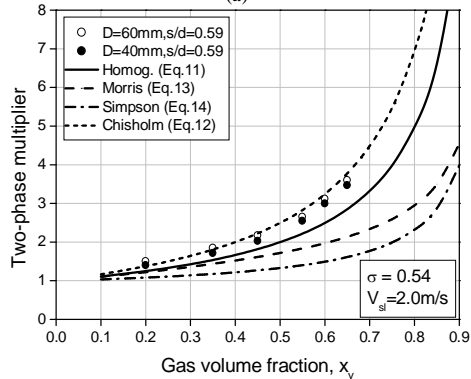
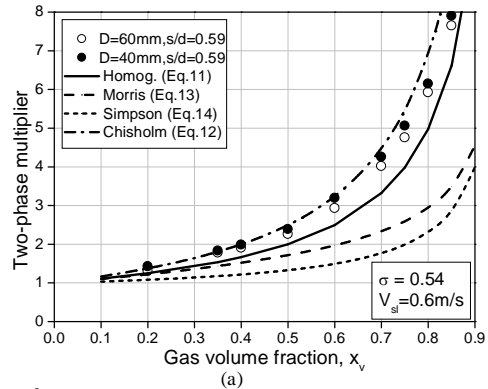


Fig. 11 Local pressure drop as a function of gas superficial velocity and orifice thickness (a)  $\sigma = 0.54$ , (b)  $\sigma = 0.73$ .



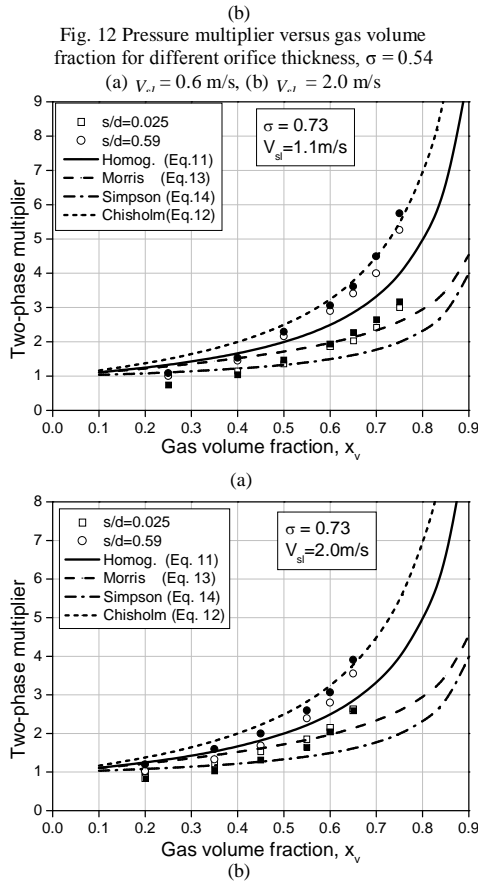


Fig. 13. Pressure multiplier versus gas volume fraction for different orifice thickness,  $\sigma = 0.73$  (a)  $V_{sl} = 1.1$  m/s, (b)  $V_{sl} = 2.0$  m/s (filled symbols for  $D = 40$  and empty symbols for  $D = 60$  mm).

superficial velocity of water and different superficial velocity of air. It can be observed that the pressure drop increases with increasing the volume fractions of air. The same trend is observed for the flow through 40 mm diameter pipe. Typical pressure drop values as a function of gas and liquid superficial velocities are shown in Fig. 11a and b where corresponding experimental (Fossa and Guglielmini [9]) values have been plotted in the same graph. It can be marked from Fig.11 that the agreement between the computation and the experimental values are pretty nice specially taking into account the complicated CFD equations those have been used to compute the pressure profiles in the present computation. It can also be observed that the effect of the orifice thickness on pressure drop is stronger with the orifice of the area flow ratio  $\sigma = 0.73$ , while the pressure drops across the orifice of the area ratio  $\sigma = 0.54$  through different orifice thicknesses are always comparable, with deviations less than 15%. Further it can be noticed that pressure drop increases with a decrease in orifice thickness irrespective of the area ratios.

The singular two-phase multiplier  $\phi_{lo}^2$  has been obtained by comparison with single phase computed pressure drops considering only liquid flow. The results are shown in Fig. 12a and b with reference to the restrictions having  $\sigma = 0.54$  and in Fig. 13a and b that refer to the larger area flow ratio constrictions of  $\sigma = 0.73$ . All these figures contain the data for both 60 mm inner diameter pipe (empty symbols) and the 40 mm inner diameter pipe (filled symbols). The numerical results for two phase multiplier are compared with the predictions of the homogeneous model (Eq. (12)), and with the values calculated by the relationships of Chisholm for thick orifices (Eq. (13) with  $B=1.5$ ), Morris (Eq. (7) and (14)) and Simpson et al. (Eq. (11) and (15)). The two-phase multiplier for thin orifices ( $s/d = 0.025$ ) are found to be quite well correlated by Morris equation. Thicker orifices ( $s/d = 0.59$ ) are characterized by higher pressure multipliers whose values are quite well fitted by the proper Chisholm formula. It can be observed from Fig. 13, the pressure multipliers pertinent to the area ratio of  $\sigma = 0.73$  show values close to unity (or even lower) when the gas volume fraction is less than about 0.5. No available relationships can account for this effect, which seems to be peculiar to these moderate flow area restrictions. The Saadawi et al. relationship (Eq. (16)) has been discarded from the present comparisons due to the fact it under predicts the numerical as well as the experimental values with differences even greater than 60%.

The main conclusion from pressure multiplier analysis is that the influence of liquid flow rate is weak. Furthermore, it can be observed that the dimensionless pressure drops obtained for  $s/d = 0.025$  (thin orifice) result in a narrow range of values. The thicker orifice ( $s/d = 0.59$ ) are characterized by higher pressure multipliers, which can show values higher than those predicted by the homogeneous model (Eq. (12)). This occurrence can be mainly ascribed to the fact that as the restriction thickness increases, the single-phase pressure drops decrease much more than the two-phase pressure drops increase at the same liquid flow rate (Fig. 10 and Fig. 11a and b). The numerical results pertinent to thick orifices are quite well fitted by Chisholm formula Eq. (13) with  $B=1.5$ , which account for orifice thickness. Finally it is evident that the pipe diameter has very little effect on the two-phase multiplier.

## V. CONCLUSIONS

1. For the flow through thin orifice ( $s/d = 0.025$ ), the vena contracta is formed outside the restriction, where as for the flow through thick orifice ( $s/d = 0.59$ ), vena contracta is always formed inside the restriction.
2. Pressure drop  $\Delta P$  across the orifice increases with a decrease in orifice thickness and pressure drop decreases with an increase in area ratio.
3. The contraction coefficient is found to be independent of the Reynolds number for values above  $5 \times 10^4$ . With turbulent flow through orifices the contraction coefficients for single phase flow of water are found to be slightly higher for contraction area ratio  $\sigma = 0.73$  than that for  $\sigma = 0.54$ .

4. In single-phase flow the contraction coefficient is found to be in good agreement with the experimental data [9] as well as with the Chisholm [3] formula predictions. The computed pressure drop across the thin orifice having thickness to diameter ratio  $s/d = 0.025$ , is more than that across thick orifice having thickness to diameter ratio  $s/d = 0.59$ .
5. The two-phase multiplier for thin orifices ( $s/d = 0.025$ ) are found to be quite well correlated by Morris equation. Thicker orifices ( $s/d = 0.59$ ) are characterized by higher pressure multipliers whose values are quite well fitted by the proper Chisholm formula.
6. The two-phase multipliers pertinent to the orifice having area ratio  $\sigma = 0.73$  show values close to unity (or even lower) when the gas volume fraction is less than about 0.5. The pipe diameter has very little effect on the two-phase multiplier.

#### REFERENCES

- [1] I. E. Idelchik, G. R. Malyavskaya, O. G. Martynenko and E. Fried, *Handbook of Hydraulic Resistances*, Boca Raton: CRC Press, 1994.
- [2] H. C. Simpson, D. H. Rooney and E. Grattan, "Two-phase Flow through Gate Valves and Orifice Plates," *Proc. Int. Conf. Physical Modelling of Multi-Phase Flow*, Coventry, 1983.
- [3] D. Chisholm, *Two-Phase Flow in Pipelines and Heat Exchangers*, London: Longman Group Ed., 1983.
- [4] S. D. Morris, "Two Phase Pressure Drop across Valves and Orifice Plates," *Proc. European Two Phase Flow Group Meeting*. Marchwood Engineering Laboratories. Southampton. UK., 1985.
- [5] M. K. Roul and S. K. Dash, "Single-Phase and Two-Phase Flow through Thin and Thick Orifices in Horizontal Pipes," *J. Fluids Eng-Trans. ASME*, DOI: 10.1115/1.4007267, 2012
- [6] Z. H. Lin, "Two Phase Flow Measurement with Sharp Edge Orifices", *Int. J. Multiphase Flow*, **8**, pp. 683-693, 1982.
- [7] A. A. Saadawi, E. Grattan and W. M. Dempster, "Two Phase Pressure Loss in Orifice Plates and Gate Valves in Large Diameter Pipes", *Proc. Celata GP*, Marco PD, Shah RK, editors. 2nd Symp. Two-Phase Flow Modelling and Experimentation. ETS. Pisa. Italy, 1999.
- [8] G. Kojasoy, M. P. Kwame, and C. T. Chang, "Two-phase Pressure Drop in Multiple Thick and Thin Orifices Plates", *Experimental Thermal and Fluid Science*, **15**, pp. 347-358, 1997.
- [9] M. Fossa, and G. Guglielmini, "Pressure Drop and Void Fraction Profiles during Horizontal Flow through Thin and Thick Orifices", *Experimental Thermal and Fluid Science*, **26**, pp. 513-523, 2002.
- [10] H. P. Grace and C. E. Lapple, "Discharge Coefficient of Small Diameter Orifices and Flow Nozzles," *Trans. ASME*, Vol. 73, pp. 639-647, 1951.
- [11] J. G. Collier and J. R. Thome, *Convective Boiling and Condensation*, New York, Oxford University Press, 1994.
- [12] S.V. Patankar, *Numerical Heat Transfer and Fluid Flow*, McGraw-Hill, Hemisphere. Washington DC, USA, 1980.
- [13] S. A. Vasquez and V. A. Ivanov, "A Phase Coupled Method for Solving Multiphase Problems on Unstructured Meshes," *Proceedings of ASME FEDSM 2000: ASME 2000 Fluids Engineering Division Summer Meeting*, Boston, Massachusetts, USA, pp. 659-664, 2000.
- [14] D. A. Drew, "Mathematical Modeling of Two-phase Flows", *Ann. Rev. Fluid Mech.*, **15**, pp. 261-291, 1983.
- [15] G. B. Wallis, *One-dimensional Two-phase Flow*, New York, McGraw Hill, 1969.
- [16] B. E. Launder and D. B. Spalding, "The Numerical Computation of Turbulent Flows", *Computer Methods in Applied Mechanics and Engineering*, **3**, pp. 269-289, 1974.